Fermilab FERMILAB-Pub-01/355-E January 2002

November 13, 2001

Υ Production and Polarization in $p\overline{p}$ Collisions at $\sqrt{s} = 1.8$ TeV

Abstract

We report on measurements of the $\Upsilon(1S)$, $\Upsilon(2S)$ and $\Upsilon(3S)$ differential cross sections $(d^2\sigma/dp_T dy)_{|y|<0.4}$, as well as on the $\Upsilon(1S)$ polarization in $p\overline{p}$ collisions at $\sqrt{s} = 1.8$ TeV using a sample of 77 ± 3 pb^{-1} collected by the Collider Detector at Fermilab. The three resonances were reconstructed through the decay $\Upsilon \to \mu^+\mu^-$. The measured angular distribution of the muons in the $\Upsilon(1S)$ rest frame is consistent with unpolarized meson production.

PACS numbers: 13.85.Ni, 14.40.Gx

D. Acosta,[13] T. Affolder,[24] H. Akimoto,[47] M. G. Albrow,[12] P. Amaral,[9] D. Ambrose,[34] D. Amidei,[26] K. Anikeev,[25] J. Antos,[1] G. Apollinari,[12] T. Arisawa,[47] A. Artikov,[10] T. Asakawa,[45] W. Ashmanskas,[9] F. Azfar,[32] P. Azzi-Bacchetta,[33] N. Bacchetta,[33] H. Bachacou,[24] S. Bailey,[17] P. de Barbaro,[38] A. Barbaro-Galtieri,[24] V. E. Barnes,[37] B. A. Barnett,[20] S. Baroiant,[5] M. Barone,[14] G. Bauer,[25] F. Bedeschi,[35] S. Belforte,[44] W. H. Bell,[16] G. Bellettini,[35] J. Bellinger,[48] D. Benjamin,[11] J. Bensinger,[4] A. Beretvas,[12] J. P. Berge,[12] J. Berryhill,[9] A. Bhatti,[39] M. Binkley,[12] D. Bisello,[33] M. Bishai,[12] R. E. Blair,[2] C. Blocker,[4] K. Bloom,[26] B. Blumenfeld,[20] S. R. Blusk,[38] A. Bocci,[39] A. Bodek,[38] G. Bolla,[37] Y. Bonushkin,[6] D. Bortoletto,[37] J. Boudreau,[36] A. Brandl,[28] S. van den Brink,[20] C. Bromberg,[27] M. Brozovic,[11] E. Brubaker,[24] N. Bruner,[28] E. Buckley-Geer,[12] J. Budagov,[10] H. S. Budd,[38] K. Burkett,[17] G. Busetto,[33] A. Byon-Wagner,[12] K. L. Byrum,[2] S. Cabrera,[11] P. Calafiura,[24] M. Campbell,[26] W. Carithers,[24] J. Carlson,[26] D. Carlsmith,[48] W. Caskey,[5] A. Castro,[3] D. Cauz,[44] A. Cerri,[35] A. W. Chan,[1] P. S. Chang,[1] P. T. Chang,[1] J. Chapman,[26]

C. Chen,[34] Y. C. Chen,[1] M. -T. Cheng,[1] M. Chertok,[5] G. Chiarelli,[35] I. Chirikov-Zorin,[10] G. Chlachidze,[10] F. Chlebana,[12] L. Christofek,[19] M. L. Chu,[1] J. Y. Chung,[30] Y. S. Chung,[38] C. I. Ciobanu,[30] A. G. Clark,[15] A. P. Colijn,[12] A. Connolly,[24] M. Convery,[39] J. Conway,[40] M. Cordelli,[14] J. Cranshaw,[42] R. Culbertson,[12] D. Dagenhart,[46] S. D'Auria,[16] F. DeJongh,[12] S. Dell'Agnello,[14] M. Dell'Orso,[35] S. Demers,[38] L. Demortier,[39] M. Deninno,[3] P. F. Derwent,[12] T. Devlin,[40] J. R. Dittmann,[12] A. Dominguez,[24] S. Donati,[35] J. Done,[41] M. D'Onofrio,[35] T. Dorigo,[17] N. Eddy,[19] K. Einsweiler,[24] J. E. Elias,[12] E. Engels, Jr.,[36] R. Erbacher,[12] D. Errede,[19] S. Errede,[19] Q. Fan,[38] H.-C. Fang,[24] R. G. Feild,[49] J. P. Fernandez,[12] C. Ferretti,[35] R. D. Field,[13] I. Fiori,[3] B. Flaugher,[12] G. W. Foster,[12] M. Franklin,[17] J. Freeman,[12] J. Friedman,[25] Y. Fukui,[23] I. Furic,[25] S. Galeotti,[35] A. Gallas,[29] M. Gallinaro,[39] T. Gao,[34] M. Garcia-Sciveres,[24] A. F. Garfinkel,[37] P. Gatti,[33] C. Gay,[49] D. W. Gerdes,[26] E. Gerstein,[8] P. Giannetti,[35] P. Giromini,[14] V. Glagolev,[10] D. Glenzinski,[12] M. Gold,[28] J. Goldstein,[12] I. Gorelov,[28] A. T. Goshaw,[11] Y. Gotra,[36] K. Goulianos,[39] C. Green,[37] G. Grim,[5] P. Gris,[12] C. Grosso-Pilcher,[9] M. Guenther,[37] G. Guillian,[26] J. Guimaraes da Costa,[17] R. M. Haas,[13] C. Haber,[24] S. R. Hahn,[12] C. Hall,[17] T. Handa,[18] R. Handler,[48] W. Hao,[42] F. Happacher,[14] K. Hara,[45] A. D. Hardman,[37] R. M. Harris,[12] F. Hartmann,[21] K. Hatakeyama,[39] J. Hauser,[6] J. Heinrich,[34] A. Heiss,[21] M. Herndon,[20] C. Hill,[5] A. Hocker,[38] K. D. Hoffman,[9] R. Hollebeek,[34] L. Holloway,[19] B. T. Huffman,[32] R. Hughes,[30] J. Huston,[27] J. Huth,[17] H. Ikeda,[45] J. Incandela,[(* 12] G. Introzzi,[35] A. Ivanov,[38] J. Iwai,[47] Y. Iwata,[18] E. James,[26] M. Jones,[34] U. Joshi,[12] H. Kambara,[15] T. Kamon,[41] T. Kaneko,[45] M. Karagoz Unel,[29] K. Karr,[46] S. Kartal,[12] H. Kasha,[49] Y. Kato,[31] T. A. Keaffaber,[37] K. Kelley,[25] M. Kelly,[26] D. Khazins,[11] T. Kikuchi,[45] B. Kilminster,[38] B. J. Kim,[22] D. H. Kim,[22] H. S. Kim,[19] M. J. Kim,[8] S. B. Kim,[22] S. H. Kim,[45] Y. K. Kim,[24] M. Kirby,[11] M. Kirk,[4] L. Kirsch,[4] S. Klimenko,[13]

P. Koehn,[30] K. Kondo,[47] J. Konigsberg,[13] A. Korn,[25] A. Korytov,[13] E. Kovacs,[2] J. Kroll,[34] M. Kruse,[11] S. E. Kuhlmann,[2] K. Kurino,[18] T. Kuwabara,[45] A. T. Laasanen,[37] N. Lai,[9] S. Lami,[39] S. Lammel,[12] J. Lancaster,[11] M. Lancaster,[24] R. Lander,[5] A. Lath,[40] G. Latino,[35] T. LeCompte,[2] K. Lee,[42] S. Leone,[35] J. D. Lewis,[12] M. Lindgren,[6] T. M. Liss,[19] J. B. Liu,[38] Y. C. Liu,[1] D. O. Litvintsev,[12] O. Lobban,[42] N. S. Lockyer,[34] J. Loken,[32] M. Loreti,[33] D. Lucchesi,[33] P. Lukens,[12] S. Lusin,[48] L. Lyons,[32] J. Lys,[24] R. Madrak,[17] K. Maeshima,[12] P. Maksimovic,[17] L. Malferrari,[3] M. Mangano,[35] M. Mariotti,[33] G. Martignon,[33] A. Martin,[49] V. Martin,[29] J. A. J. Matthews,[28] P. Mazzanti,[3] K. S. McFarland,[38] P. McIntyre,[41] M. Menguzzato,[33] A. Menzione,[35] P. Merkel,[12] C. Mesropian,[39] A. Meyer,[12] T. Miao,[12] R. Miller,[27] J. S. Miller,[26] H. Minato,[45] S. Miscetti,[14] M. Mishina,[23] G. Mitselmakher,[13] Y. Miyazaki,[31] N. Moggi,[3] E. Moore,[28] R. Moore,[26] Y. Morita,[23] T. Moulik,[37] M. Mulhearn,[25] A. Mukherjee,[12] T. Muller,[21] A. Munar,[35] P. Murat,[12] S. Murgia,[27] J. Nachtman,[6] V. Nagaslaev,[42] S. Nahn,[49] H. Nakada,[45] I. Nakano,[18] C. Nelson,[12] T. Nelson,[12] C. Neu,[30] D. Neuberger,[21] C. Newman-Holmes,[12] C.-Y. P. Ngan,[25] H. Niu,[4] L. Nodulman,[2] A. Nomerotski,[13] S. H. Oh,[11] Y. D. Oh,[22] T. Ohmoto,[18] T. Ohsugi,[18] R. Oishi,[45] T. Okusawa,[31] J. Olsen,[48] W. Orejudos,[24] C. Pagliarone,[35] F. Palmonari,[35] R. Paoletti,[35] V. Papadimitriou,[42] D. Partos,[4] J. Patrick,[12] G. Pauletta,[44] M. Paulini,[8] C. Paus,[25] D. Pellett,[5] L. Pescara,[33] T. J. Phillips,[11] G. Piacentino,[35] K. T. Pitts,[19] A. Pompos,[37] L. Pondrom,[48] G. Pope,[36] F. Prokoshin,[10] J. Proudfoot,[2] F. Ptohos,[14] O. Pukhov,[10] G. Punzi,[35] A. Rakitine,[25] F. Ratnikov,[40] D. Reher,[24] A. Reichold,[32] P. Renton,[32] A. Ribon,[33] W. Riegler,[17] F. Rimondi,[3] L. Ristori,[35] M. Riveline,[43] W. J. Robertson,[11] T. Rodrigo,[7] S. Rolli,[46] L. Rosenson,[25] R. Roser,[12] R. Rossin,[33] C. Rott,[37] A. Roy,[37] A. Ruiz,[7] A. Safonov,[5] R. St. Denis,[16] W. K. Sakumoto,[38] D. Saltzberg,[6] C. Sanchez,[30] A. Sansoni,[14] L. Santi,[44] H. Sato,[45] P. Savard,[43] A. Savoy-Navarro,[12] P. Schlabach,[12] E. E. Schmidt,[12]

M. P. Schmidt,[49] M. Schmitt,[29] L. Scodellaro,[33] A. Scott,[6] A. Scribano,[35] A. Sedov,[37] S. Segler,[12] S. Seidel,[28] Y. Seiya,[45] A. Semenov,[10] F. Semeria,[3] T. Shah,[25] M. D. Shapiro,[24] P. F. Shepard,[36] T. Shibayama,[45] M. Shimojima,[45] M. Shochet,[9] A. Sidoti,[33] J. Siegrist,[24] A. Sill,[42] P. Sinervo,[43] P. Singh,[19] A. J. Slaughter,[49] K. Sliwa,[46] C. Smith,[20] F. D. Snider,[12] A. Solodsky,[39] J. Spalding,[12] T. Speer,[15] P. Sphicas,[25] F. Spinella,[35] M. Spiropulu,[9] L. Spiegel,[12] J. Steele,[48] A. Stefanini,[35] J. Strologas,[19] F. Strumia, [15] D. Stuart,[12] K. Sumorok,[25] T. Suzuki,[45] T. Takano,[31] R. Takashima,[18] K. Takikawa,[45] P. Tamburello,[11] M. Tanaka,[45] B. Tannenbaum,[6] M. Tecchio,[26] R. J. Tesarek,[12] P. K. Teng,[1] K. Terashi,[39] S. Tether,[25] A. S. Thompson,[16] E. Thomson,[30] R. Thurman-Keup,[2] P. Tipton,[38] S. Tkaczyk,[12] D. Toback,[41] K. Tollefson,[38] A. Tollestrup,[12] D. Tonelli,[35] H. Toyoda,[31] W. Trischuk,[43] J. F. de Troconiz,[17] J. Tseng,[25] D. Tsybychev,[13] N. Turini,[35] F. Ukegawa,[45] T. Vaiciulis,[38] J. Valls,[40] E. Vataga,[35] S. Vejcik III,[12] G. Velev,[12] G. Veramendi,[24] R. Vidal,[12] I. Vila,[7] R. Vilar,[7] I. Volobouev,[24] M. von der Mey,[6] D. Vucinic,[25] R. G. Wagner,[2] R. L. Wagner,[12] N. B. Wallace,[40] Z. Wan,[40] C. Wang,[11] M. J. Wang,[1] S. M. Wang,[13] B. Ward,[16] S. Waschke,[16] T. Watanabe,[45] D. Waters,[32] T. Watts,[40] R. Webb,[41] H. Wenzel,[21] W. C. Wester III,[12] A. B. Wicklund,[2] E. Wicklund,[12] T. Wilkes,[5] H. H. Williams,[34] P. Wilson,[12] B. L. Winer,[30] D. Winn,[26] S. Wolbers,[12] D. Wolinski,[26] J. Wolinski,[27] S. Wolinski,[26] S. Worm,[40] X. Wu,[15] J. Wyss,[35] W. Yao,[24] G. P. Yeh,[12] P. Yeh,[1] J. Yoh,[12] C. Yosef,[27] T. Yoshida,[31] I. Yu,[22] S. Yu,[34] Z. Yu,[49] A. Zanetti,[44] F. Zetti,[24] and S. Zucchelli[3]

(CDF Collaboration)

[1] *Institute of Physics, Academia Sinica, Taipei, Taiwan 11529, Republic of China*

[2] *Argonne National Laboratory, Argonne, Illinois 60439*

[3] *Istituto Nazionale di Fisica Nucleare, University of Bologna, I-40127 Bologna, Italy*

[4] *Brandeis University, Waltham, Massachusetts 02254*

[5] *University of California at Davis, Davis, California 95616*

[6] *University of California at Los Angeles, Los Angeles, California 90024*

[7] *Instituto de Fisica de Cantabria, CSIC-University of Cantabria, 39005 Santander, Spain*

[8] *Carnegie Mellon University, Pittsburgh, PA 15218*

[9] *Enrico Fermi Institute, University of Chicago, Chicago, Illinois 60637*

[10] *Joint Institute for Nuclear Research, RU-141980 Dubna, Russia*

[11] *Duke University, Durham, North Carolina 27708*

[12] *Fermi National Accelerator Laboratory, Batavia, Illinois 60510*

[13] *University of Florida, Gainesville, Florida 32611*

[14] *Laboratori Nazionali di Frascati, Istituto Nazionale di Fisica Nucleare, I-00044 Frascati, Italy*

[15] *University of Geneva, CH-1211 Geneva 4, Switzerland*

[16] *Glasgow University, Glasgow G12 8QQ, United Kingdom*

[17] *Harvard University, Cambridge, Massachusetts 02138*

[18] *Hiroshima University, Higashi-Hiroshima 724, Japan*

[19] *University of Illinois, Urbana, Illinois 61801*

[20] *The Johns Hopkins University, Baltimore, Maryland 21218*

[21] *Institut für Experimentelle Kernphysik, Universität Karlsruhe, 76128 Karlsruhe, Germany*

[22] *Center for High Energy Physics: Kyungpook National University, Taegu 702-701; Seoul National University, Seoul 151-742; and SungKyunKwan University, Suwon 440-746; Korea*

[23] *High Energy Accelerator Research Organization (KEK), Tsukuba, Ibaraki 305, Japan*

[24] *Ernest Orlando Lawrence Berkeley National Laboratory, Berkeley, California 94720*

[25] *Massachusetts Institute of Technology, Cambridge, Massachusetts 02139*

[26] *University of Michigan, Ann Arbor, Michigan 48109*

[27] Michigan State University, East Lansing, Michigan 48824

[28] University of New Mexico, Albuquerque, New Mexico 87131

[29] Northwestern University, Evanston, Illinois 60208

[30] The Ohio State University, Columbus, Ohio 43210

[31] Osaka City University, Osaka 588, Japan

[32] University of Oxford, Oxford OX1 3RH, United Kingdom

[33] Universita di Padova, Istituto Nazionale di Fisica Nucleare, Sezione di Padova, I-35131 Padova, Italy

[34] University of Pennsylvania, Philadelphia, Pennsylvania 19104

[35] Istituto Nazionale di Fisica Nucleare, University and Scuola Normale Superiore of Pisa, I-56100 Pisa, Italy

[36] University of Pittsburgh, Pittsburgh, Pennsylvania 15260

[37] Purdue University, West Lafayette, Indiana 47907

[38] University of Rochester, Rochester, New York 14627

[39] Rockefeller University, New York, New York 10021

[40] Rutgers University, Piscataway, New Jersey 08855

[41] Texas A&M University, College Station, Texas 77843

[42] Texas Tech University, Lubbock, Texas 79409

[43] Institute of Particle Physics, University of Toronto, Toronto M5S 1A7, Canada

[44] Istituto Nazionale di Fisica Nucleare, University of Trieste/ Udine, Italy

[45] University of Tsukuba, Tsukuba, Ibaraki 305, Japan

[46] Tufts University, Medford, Massachusetts 02155

[47] Waseda University, Tokyo 169, Japan

[48] University of Wisconsin, Madison, Wisconsin 53706

[49] Yale University, New Haven, Connecticut 06520

[(*)] Now at University of California, Santa Barbara, California 93106

We report on a study of the reaction $p\bar{p} \rightarrow \Upsilon X \rightarrow \mu^+\mu^- X$ at $\sqrt{s} = 1.8$ TeV. This study yields the transverse momentum (p_T) dependence of the cross sections for the production of the Υ(1S), Υ(2S), and Υ(3S) states as well as the Υ(1S) polarization. Both the cross section and polarization measurements are important for the investigation of $q\overline{q}$ bound state production mechanisms in $p\bar{p}$ collisions [1]. In our previous Υ analysis [2], based on a 16.6 $\pm$ 0.6 pb^{-1} data sample, the differential cross sections were seen to disagree both in shape and magnitude with theoretical predictions using only color singlet matrix elements in the NRQCD (non-relativistic quantumchromodynamics) factorization formalism [3]. Similarly, our measurements of the prompt J/ψ and ψ(2S) charmonium production cross sections [4] were found to be an order of magnitude higher than the theoretical predictions [5, 6, 7].

These initial measurements sparked renewed theoretical efforts focusing on mechanisms that allow intermediate color octet $c\overline{c}$ and $b\overline{b}$ states to be produced and evolve to the observed quarkonium mesons [3, 5, 8, 9]. These models can accommodate the quarkonia cross section measurements from the Tevatron. In addition, the inclusion of color octet matrix elements in the NRQCD factorization formalism leads to predictions of transversely polarized quarkonium production at high transverse momentum ($p_T \gg \mathrm{M}_{Q\bar{Q}}$) due to the predominance of nearly on-shell gluon fragmentation into $q\overline{q}$ pairs [10, 11]. Subsequent measurements from CDF on prompt J/ψ and ψ(2S) production polarization [12] cannot distinguish between the competing theories but tend to disfavor the polarization predictions of references [10] and [11]. In this paper we present studies of the Υ system to further the investigation of different theoretical descriptions of heavy quarkonia production.

We present measurements of the differential cross section $(d^2\sigma/dp_T dy) \times Br(\Upsilon \rightarrow \mu^+\mu^-)$ for values of Υ rapidity $|y| < 0.4$ (where $y = \frac{1}{2} \cdot \ln(\frac{E+p_{||}}{E-p_{||}})$, E is the energy of the dimuon pair, and $p_{||}$ its momentum parallel to the beam direction) in the p_T interval $0 < p_T(\Upsilon) < 20$ GeV/c

for the Υ(1S), Υ(2S), and Υ(3S) states. Due to the increased size of the current data sample we are able to measure the shape of the Υ(2S) and Υ(3S) differential cross sections much more accurately than in our previous analysis. The measurements of the Υ cross sections allow for exploration of the low p_T production region inaccessible in the charmonium cross section measurements which do not extend below 4 GeV/c due to triggering constraints. In addition, we present the production polarization of the Υ(1S) state for $0 < p_T(\Upsilon) < 20$ GeV/c, the first such measurement from a hadron collider.

The data were collected in 1993-95 by the Collider Detector at Fermilab and correspond to an integrated luminosity of 77 ± 3 pb^{-1}. The CDF detector has been described in detail elsewhere [13]. The components relevant to this analysis are briefly described here. The z-axis of the detector coordinate system is along the beam direction. The Central Tracking Chamber (CTC) is in a 1.4 T axial magnetic field and has a resolution of $\delta p_T/p_T = \sqrt{(0.0011 p_T)^2 + (0.0066)^2}$ for tracks constrained to come from the beam line, where p_T is measured in GeV/c. The central muon chambers (CMU) are located at a radius of 3.5 m from the beam axis behind five interaction lengths of calorimeter and provide muon identification in the region of pseudorapidity $|\eta| < 0.6$, where $\eta = -\ln[\tan(\theta/2)]$ and θ is the polar angle with respect to the beam axis. Outside the CMU we have installed the central muon upgrade system (CMP) which consists of four layers of drift chambers behind an additional four interaction lengths of steel absorber.

The measurements reported here are based on a data sample of muon pairs collected with a three level trigger. The first level trigger required two charged track segments in the central muon chambers. The efficiency for this trigger rises from 40% at $p_T = 1.5$ GeV/c to 93% for muons of $p_T > 3.0$ GeV/c. The second level trigger required at least one muon segment to match a CTC track found by the hardware fast track processor (CFT). The CFT performed a limited reconstruction of charged tracks considering only those with p_T above 2 GeV/c. Muon candidates found by the first level trigger were required to match a CFT track within about 5 degrees in azimuth. The Level 2 trigger had an average efficiency of 95% for muons with $p_T > 2.5$ GeV/c. The third level trigger performed three dimensional track reconstruction and accepted muon pairs with an invariant mass in the region 8.5 to 11.4 GeV/c^2.

Additional requirements were made to isolate the Υ resonances. Both muons from the $\Upsilon \to \mu^+\mu^-$ decay were required to be identified by the CMU system and at least one muon had to be identified by the CMP system. The momentum of each muon was determined using CTC information along with the constraint that the particles must originate from the beamline. To reduce the sensitivity to the trigger thresholds, the p_T of each muon was required to be greater than 2.2 GeV/c. Each muon chamber track was required to match the extrapolation of a CTC track to within 3σ in r- ϕ and 3.5σ in z, where σ is the calculated uncertainty due to multiple scattering and measurement uncertainties. The muons were required to have opposite charge and the rapidity of the reconstructed pair had to be in the CMU fiducial rapidity region $|y| < 0.4$. The transverse momentum of the reconstructed pair was required to be in the region $0 < p_T < 20$ GeV/c. The resulting mass distribution of muon pairs is shown in Figure 1.

The differential cross section times the branching ratio for $\Upsilon \to \mu^+\mu^-$ is calculated in each p_T bin according to the equation

$$\left(\frac{d^2\sigma(\Upsilon)}{dp_T dy}\right)_{|y|<0.4} Br(\Upsilon \to \mu^+\mu^-) = \frac{N_{fit}}{A\,(\int \mathcal{L}dt)\,\Delta p_T\,\Delta y\,\epsilon_{trig}\,\epsilon_{l3}\,\epsilon_{trk}\,\epsilon_{\mu}\,\epsilon_{rad}\,\epsilon_{norm}}$$

where N_{fit} is the number of Υ signal events in each p_T bin, A is the geometric and kinematic acceptance, $\int \mathcal{L}dt$ is the integrated luminosity, Δp_T is the width of the bin, and Δy is the rapidity range of the Υ production. The various efficiency corrections include the combined first and second level trigger efficiency ϵ_{trig}, the third level trigger efficiency ϵ_{l3}, the efficiency for reconstructing both tracks in the CTC ϵ_{trk}, and the efficiency for reconstructing both muon track segments and associating them with extrapolated CTC tracks ϵ_{μ}. The additional efficiency correction factor ϵ_{rad} accounts for an under counting of events due to internal radiation from the muons distorting the Gaussian shapes assumed in the determination of N_{fit} as described below. The efficiency correction factor ϵ_{norm} accounts for a loss of events seen as a function of instantaneous luminosity during the run [16].

We used a binned maximum likelihood fit on the dimuon mass distribution in each p_T bin to determine the number of signal events (N_{fit}). In order to estimate the background accurately, the values of N_{fit} for each resonance were obtained by fitting all three resonances simultaneously to Gaussian shapes with a quadratic background. The relative widths of the resonances in each p_T bin were constrained to values determined from a Monte Carlo simulation.

The event yields were corrected for the first and second level trigger efficiency ϵ_{trig} which was typically 75% for each p_T bin. The remaining efficiencies were measured to be independent of p_T and are $\epsilon_{l3} = (97 \pm 2)\%$, $\epsilon_{trk} = (98 \pm 2)\%$, $\epsilon_{\mu} = (95 \pm 1)\%$, $\epsilon_{rad} = (93 \pm 2)\%$ and $\epsilon_{norm} = (88 \pm 4)\%$. The various efficiencies were measured using both Monte Carlo methods and several independent calibration data sets.

The geometric and kinematic acceptances for Υ(1S), Υ(2S), Υ(3S) $\rightarrow \mu^+\mu^-$ were calculated using the Monte Carlo simulation. The event generator produced Υ particles with flat p_T and y distributions. Since the polarization of Υ production was not known, the states were assumed to decay isotropically in the Υ rest frame. In addition we generated event sets with transverse and longitudinal polarization in order to measure the Υ(1S) polarization and to set systematic uncertainties on the other cross section measurements. Once the Υ p_T spectrum was measured, the Monte Carlo events were reweighted according to the measured p_T distribution for polarization acceptance measurements and systematic uncertainty studies. The generated events were processed with a detector simulation and the same reconstruction criteria that were imposed on the data. The integrated acceptance A was found to be similar for each of the three resonances and varied as a function of p_T from 17% to 24%.

Systematic uncertainties on the cross section measurements arise from the luminosity determination (4.1%), the level 1 and level 2 trigger efficiency corrections ϵ_{trig} (4%), and from the remaining efficiency corrections (6%). A p_T dependent systematic uncertainty arises from the unknown polarization for the Υ(2S) and Υ(3S) states. This uncertainty was determined by computing the kinematic acceptances assuming all the Υ mesons were produced with either transverse or longitudinal polarization. The Υ(1S) acceptance uncertainty was also evaluated by varying the Monte Carlo polarization within the measured errors on this quantity yielding no significant change in the cross section value. Hence, no additional systematic error was assigned to the Υ(1S) cross section measurement due to uncertainties in the polarization model.

The differential cross section results are summarized in Tables I–III. The polarization systematic uncertainties are indicated separately from the other systematic uncertainties which have been added in quadrature. The cross sections are displayed in Figure 2 where each of the differential cross sections has been normalized by its integrated value. The vertical error bars represent the statistical uncertainty only. The production cross sections for the Υ(1S), Υ(2S) and Υ(3S) are seen to have the same shape as a function of Υ transverse momentum. We note this is expected by the Soft Color model of quarkonium production [9]. We also note that fits of color singlet and octet matrix elements in the NRQCD factorization formalism describe the shape and magnitude of the three Υ cross sections [17, 18].

We have also performed a polarization analysis on the $\Upsilon(1S)$ data sample by studying the angle between the direction of the μ^+ in the $\Upsilon(1S)$ rest frame and the Υ direction in the $p\bar{p}$ center-of-mass frame. For this study, the muons from the Υ decay were assumed to have an angular distribution proportional to $1 + \alpha\cos^2\theta^*$ where θ^* is the polar angle in the rest frame of the Υ and α can vary between ± 1. A value of $+1$ corresponds to transversely polarized production and a value of -1 corresponds to longitudinally polarized production.

The polarization measurement is made by fitting the shape of the uncorrected data in the variable $\cos\theta^*$ to templates for transversely and longitudinally polarized production derived from the Monte Carlo simulation yielding the longitudinally polarized fraction $\Gamma_L/\Gamma \equiv \eta$. The relationship between η and α is given by $\alpha = (1 - 3\eta)/(1 + \eta)$.

Separate χ^2 fits of combinations of longitudinally and transversely polarized Monte Carlo templates to the data in the $|y| < 0.4$ region and in the range $0 < p_T < 20$ GeV/c yield the $\Upsilon(1S)$ polarization in four separate transverse momentum intervals. The measurements in all four p_T regions are consistent with unpolarized $\Upsilon(1S)$ production and are summarized in Table IV. In the highest transverse momentum region $8 < p_T < 20$ GeV/c, the longitudinal fraction is measured to be $\Gamma_L/\Gamma = 0.39 \pm 0.11$ ($\alpha = -0.12 \pm 0.22$). This result is in agreement with the polarization calculated within the NRQCD factorization framework in reference [19]. In Figure 3 we display the $\cos\theta^*$ distribution for this highest transverse momentum region. The number of events in each $\cos\theta^*$ bin were counted by fitting the dimuon Υ invariant mass distribution in that bin. The points represent the data while the solid line is the result of the fit to the Monte Carlo distributions.

In conclusion we have measured the differential cross sections in the range $0 < p_T < 20$ GeV/c for the $\Upsilon(1S)$, $\Upsilon(2S)$ and $\Upsilon(3S)$ states and the $\Upsilon(1S)$ polarization. The rates of production were measured to be lower than, but compatible with, the ones reported in [2].

Fits of NRQCD matrix elements can describe the cross sections but their validity can only be determined by confrontation with other experiments. We have also found that the $\Upsilon(1S)$ data are consistent with unpolarized production in the region $0 < p_T < 20$ GeV/c consistent with all current models of Υ production.

We thank the Fermilab staff and the technical staffs of the participating institutions for their vital contributions. This work was supported by the U.S. Department of Energy and National Science Foundation; the Italian Istituto Nazionale di Fisica Nucleare; the Ministry of Education, Culture, Sports, Science, and Technology of Japan; the Natural Sciences and Engineering Research Council of Canada; the National Science Council of the Republic of China; the Swiss National Science Foundation; the A. P. Sloan Foundation; the Bundesministerium fuer Bildung und Forschung, Germany; the Korea Science and Engineering Foundation (KoSEF); the Korea Research Foundation; and the Comision Interministerial de Ciencia y Tecnologia, Spain.

References

[1] R. Baier and R. Rückl, Z. Phys. C **19**, 251 (1983).

[2] F. Abe *et al.*, Phys. Rev. Lett. **75**, 4358 (1995).

[3] P. Cho and A. K. Leibovich, Phys. Rev. D **53**, 150 (1996); P. Cho and A. K. Leibovich, Phys. Rev. D **53**, 6203 (1996).

[4] F. Abe *et al.*, Phys. Rev. Lett. **79**, 572 (1997); F. Abe *et al.*, Phys. Rev. Lett. **79**, 578 (1997).

[5] D.P. Roy and K. Sridhar, Phys. Lett. B **339**, 141 (1994).

[6] M. Cacciari and M. Greco, Phys. Rev. Lett. **73**, 1586 (1994).

[7] E. Braaten *et al.*, Phys. Lett. B **333**, 548 (1994).

[8] R. Gavai *et al.*, Int. J. Mod. Phys. A **10**, 3043, (1995).

[9] J. F. Amundson *et al.*, Phys. Lett. B **390**, 323 (1997).

[10] E. Braaten, B. Kniehl and J. Lee, Phys. Rev. D **62**, 094005 (2000).

[11] M. Beneke and M. Krämer, Phys. Rev. D **55**, 5269 (1997).

[12] T. Affolder *et al.*, Phys. Rev. Lett. **85**, 2886 (2000).

[13] F. Abe *et al.*, Nucl. Instrum. Methods A **271**, 387 (1988).

[14] E. Braaten and S. Fleming, Phys. Rev. Lett. **74**, 3327 (1995).

[15] C. Caso *et al.*, Particle Data Group, Eur. Phys. J. C **15**, 1 (2000).

[16] D. Acosta *et al.*, submitted to Phys. Rev. D, FERMILAB-PUB-01/347-E, November 2001.

[17] E. Braaten, S. Fleming and A. K. Leibovich, Phys. Rev. D **63**, 094006 (2001).

[18] J.L. Domenech-Garret and M.A. Sanchis-Lozano, Nucl. Phys. **B601**, 395 (2001).

[19] E. Braaten and J. Lee, Phys. Rev. D **63**, 071501(R) (2001).

Table I: The differential cross section $(d^2\sigma/dp_T dy)_{|y|<0.4} \times Br(\Upsilon \to \mu^+\mu^-)$ for Υ(1S).

p_T Range GeV/c	Mean p_T GeV/c	Cross Section pb/(GeV/c)	Stat. Error pb/(GeV/c)	Syst. Error pb/(GeV/c)
0-0.5	0.29	17.8	$\pm$ 3.6	$\pm$ 1.5
0.5-1	0.77	50.6	$\pm$ 5.7	$\pm$ 4.1
1-2	1.5	89.6	$\pm$ 5.7	$\pm$ 7.3
2-3	2.5	114.4	$\pm$ 6.5	$\pm$ 9.4
3-4	3.5	99.1	$\pm$ 6.0	$\pm$ 8.1
4-5	4.5	86.8	$\pm$ 5.7	$\pm$ 7.1
5-6	5.5	69.7	$\pm$ 4.8	$\pm$ 5.7
6-7	6.5	46.4	$\pm$ 3.7	$\pm$ 3.8
7-8	7.5	39.0	$\pm$ 3.2	$\pm$ 3.2
8-9	8.4	29.9	$\pm$ 2.9	$\pm$ 2.4
9-10	9.4	22.1	$\pm$ 2.4	$\pm$ 1.8
10-12	10.9	12.0	$\pm$ 1.2	$\pm$ 1.0
12-16	13.7	5.2	$\pm$ 0.5	$\pm$ 0.4
16-20	17.5	1.1	$\pm$ 0.2	$\pm$ 0.1

Table II: The differential cross section $(d^2\sigma/dp_T dy)_{|y|<0.4} \times Br(\Upsilon \to \mu^+\mu^-)$ for Υ(2S).

p_T Range GeV/c	Mean p_T GeV/c	Cross Section pb/(GeV/c)	Stat. Error pb/(GeV/c)	Pol. Syst. Error pb/(GeV/c)	Other Syst. Error pb/(GeV/c)
0-1	0.62	10.4	± 2.3	± 2.2	± 0.9
1-2	1.5	22.6	± 3.3	± 2.1	± 1.8
2-3	2.5	22.7	± 3.3	± 0.9	± 1.9
3-4	3.5	21.6	± 3.5	± 0.5	± 1.8
4-6	4.9	20.0	± 2.5	± 1.4	± 1.6
6-8	6.9	12.0	± 1.6	± 1.3	± 1.0
8-10	8.9	7.3	± 1.2	± 0.2	± 0.6
10-14	11.6	3.2	± 0.5	± 0.4	± 0.3
14-20	16.5	1.1	± 0.2	± 0.2	± 0.1

Table III: The differential cross section $(d^2\sigma/dp_T dy)_{|y|<0.4} \times Br(\Upsilon \rightarrow \mu^+\mu^-)$ for Υ(3S).

p_T Range GeV/c	Mean p_T GeV/c	Cross Section pb/(GeV/c)	Stat. Error pb/(GeV/c)	Pol. Syst. Error pb/(GeV/c)	Other Syst. Error pb/(GeV/c)
0-1	0.58	6.2	± 1.9	± 1.1	± 0.5
1-2	1.6	10.3	± 2.7	± 0.9	± 0.8
2-3	2.5	12.7	± 2.9	± 0.1	± 1.1
3-4	3.5	14.4	± 3.3	± 1.8	± 1.2
4-6	4.9	9.7	± 2.0	± 1.0	± 0.8
6-8	6.9	5.8	± 1.5	± 0.6	± 0.5
8-10	8.8	5.8	± 1.2	± 0.4	± 0.5
10-14	11.6	2.1	± 0.5	± 0.2	± 0.2
14-20	15.8	0.4	± 0.1	± 0.1	± 0.04

Table IV: $\Upsilon(1S)$ polarization results for $|y| < 0.4$.

p_T (GeV/c)	$,_L/,$	α
$0.0 - 3.0$	0.31 ± 0.06	$+0.05 \pm 0.14$
$3.0 - 5.0$	0.33 ± 0.06	$+0.01 \pm 0.14$
$5.0 - 8.0$	0.29 ± 0.07	$+0.10 \pm 0.17$
$8.0 - 20.0$	0.39 ± 0.11	-0.12 ± 0.22

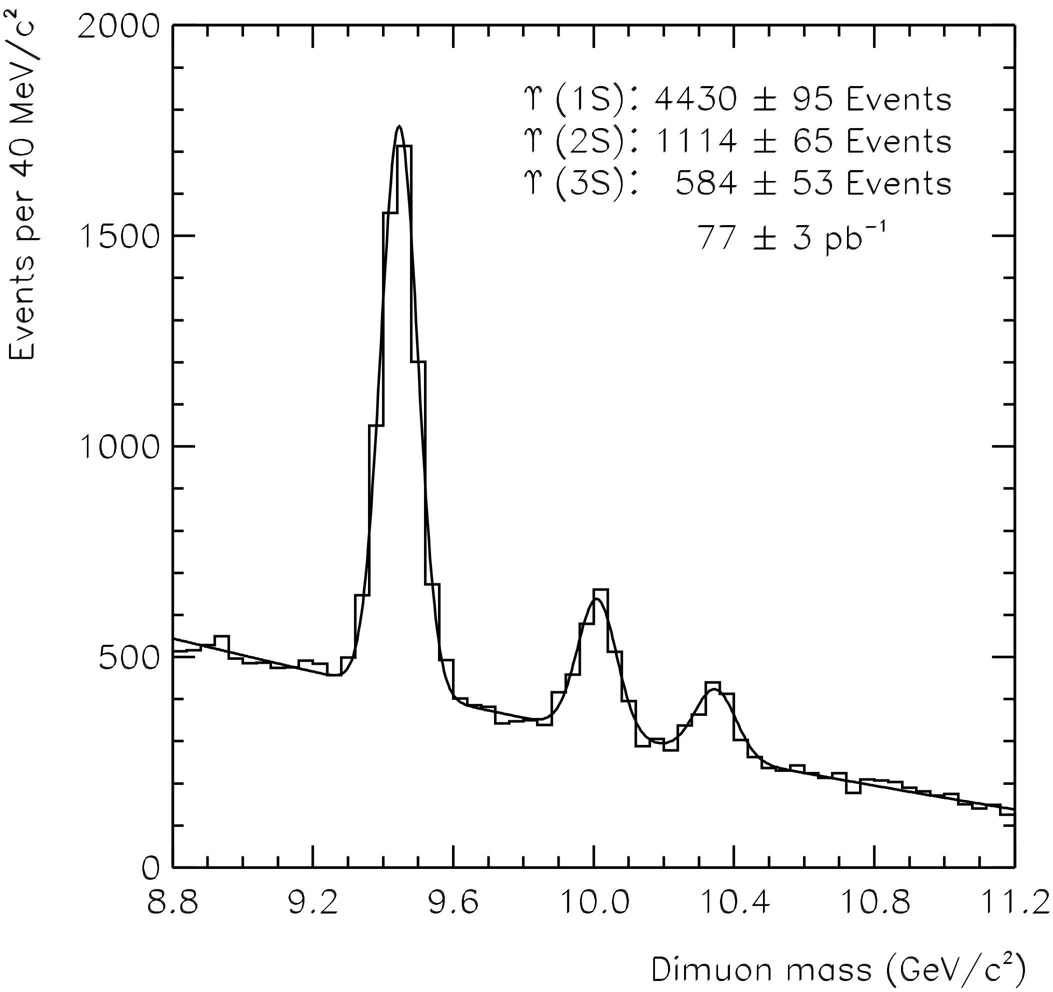

Figure 1: The invariant mass distribution of opposite sign muon pairs in the Υ mass region for $|y| < 0.4$. The histogram corresponds to the data and the solid curve represents a Gaussian fit to each resonance plus a quadratic background.

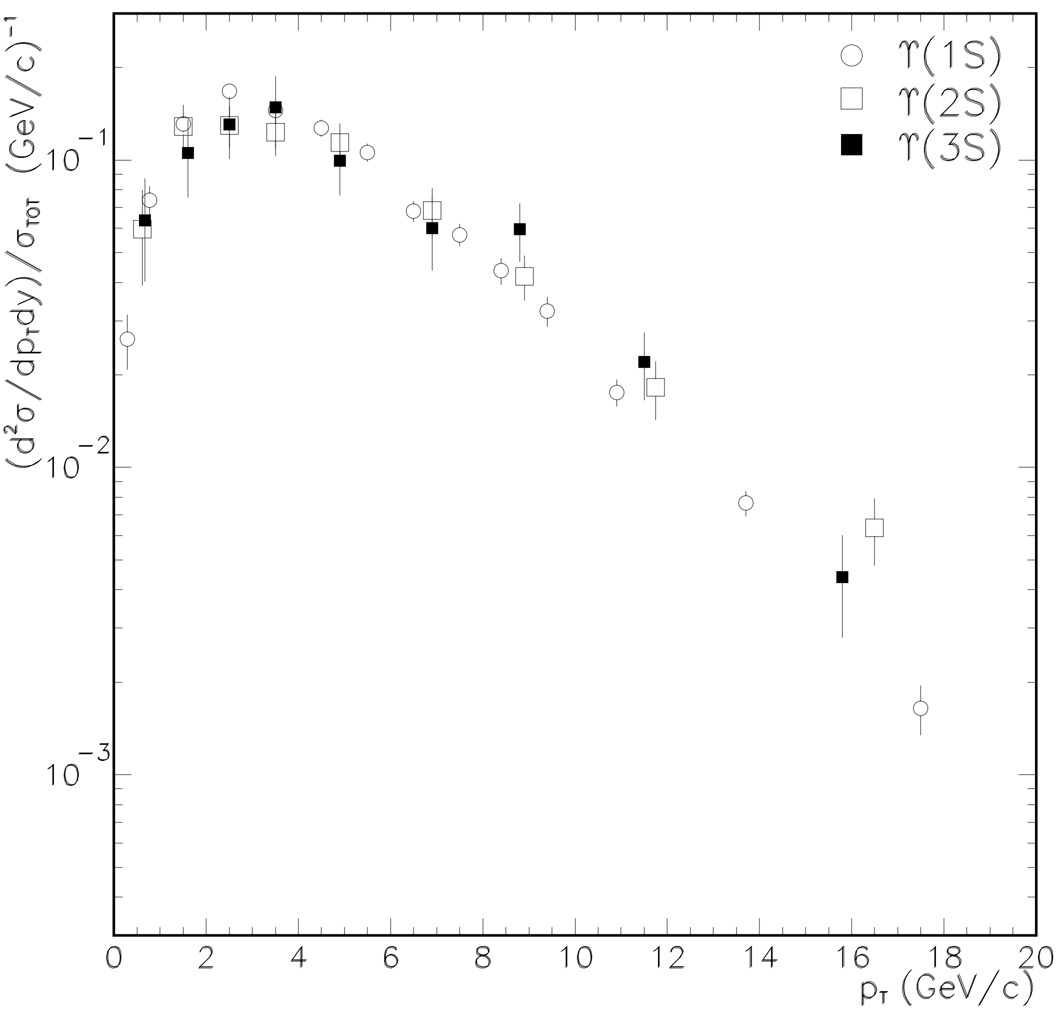

Figure 2: The product $\frac{1}{\sigma_{TOT}}(d^2\sigma/dp_T dy)_{|y|<0.4}$ vs. p_T for $\Upsilon(1S) \to \mu^+\mu^-$, $\Upsilon(2S) \to \mu^+\mu^-$ and $\Upsilon(3S) \to \mu^+\mu^-$. The vertical error bars indicate the statistical uncertainty only. Each differential cross section has been normalized by its integrated value.

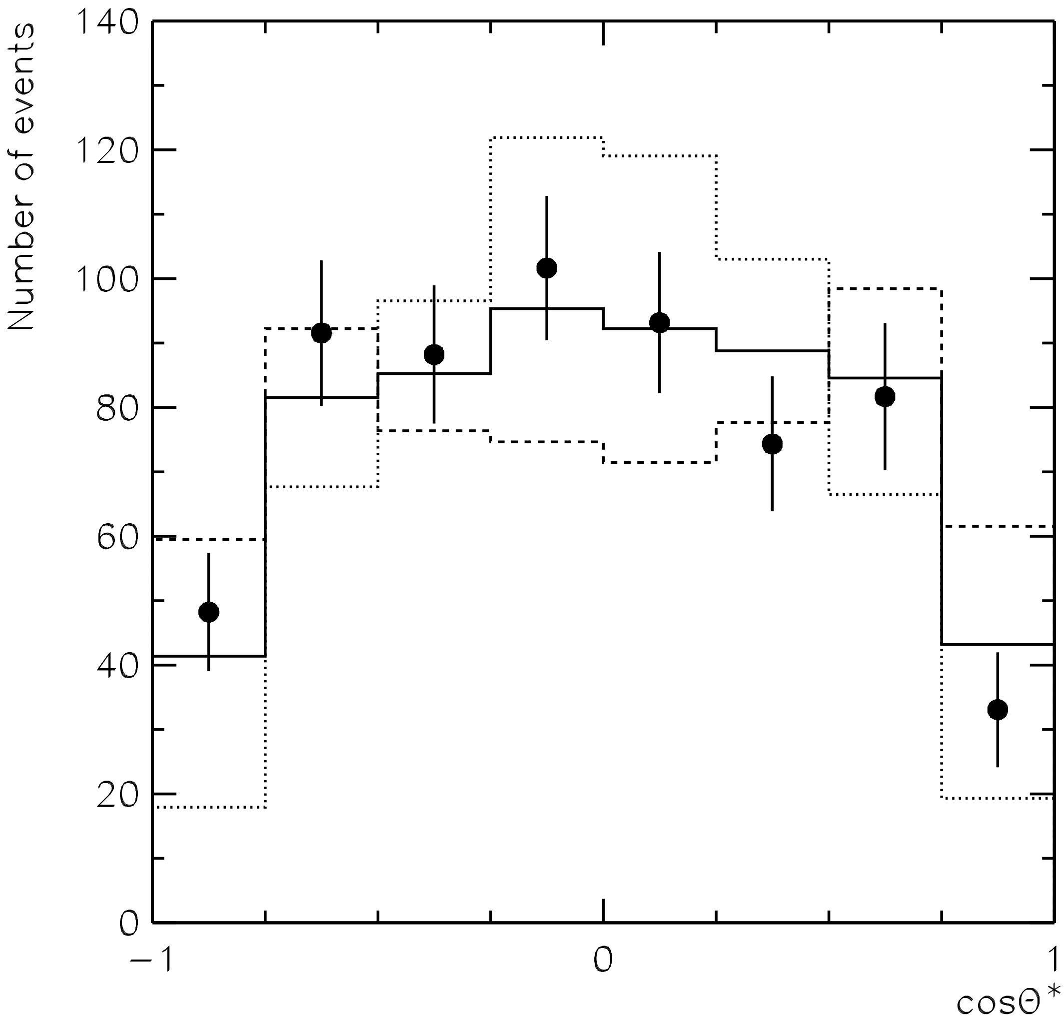

Figure 3: The uncorrected $\cos\theta^*$ distribution for $|y| < 0.4$ and $8 < p_T < 20$ GeV/c. The solid points represent the data. The solid line represents the combined fit of the longitudinally and transversely polarized Monte Carlo templates to the data. The dotted (dashed) histogram represents the longitudinally (transversely) polarized Monte Carlo template normalized individually to the total number of data events.